ELSEVIER

Mechanics of Materials 23 (1996) 169–189

MECHANICS OF MATERIALS

Stress fields due to dislocation walls in infinite and semi-infinite bodies

V.A. Lubarda and D.A. Kouris

Department of Mechanical and Aerospace Engineering, Arizona State University, Tempe, AZ 85287-6106, USA

Received 25 May 1995

Abstract

Stress fields due to dislocation walls in infinite and semi-infinite bodies are derived. Finite, infinite, and semi-infinite walls of identical edge dislocations with uniform spacing are considered. The results corresponding to walls with discrete dislocation distributions are compared to those of the walls with continuous distribution of infinitesimal dislocations. The stress relaxation effects produced by the free surface in the neighborhood of a dislocation wall are studied. It is shown that the long range stresses are exerted by bounded walls in both infinite and semi-infinite bodies. The stress divergence or its absence is discussed for various wall configurations.

1. Introduction

A study of the elastic stress field due to dislocation walls and other organized dislocation structures has recently received a revived attention (Lubarda et al., 1993; Saada and Bouchaud, 1993). Dislocation walls have been extensively used in the past to model the grain boundaries and sub-boundaries in crystals. They have been used to explain the occurrence of polygonalization and kink bands (Nabarro, 1967), epitaxial growth (Pond, 1989), persistent slip bands in fatigued specimens (Laird, 1983), dislocation cell structure (Amodeo and Ghoniem, 1990), etc. A comprehensive treatment of grain boundary modeling by various planar dislocation networks and dislocation walls is given by Hirth and Lothe (1968). Li (1972) suggested a grain boundary model that consisted of the wall of wedge dislocation or disclination dipoles. Rey and Saada (1975) and Saada (1979) further analyzed the elastic fields of periodic dislocation structures by using the concept of dislocation density tensor and continuum distribution of dislocations. Mura (1989) introduced a concept of impotent dislocation walls, which exert no stresses and displacements in the body, and have a possible application to dislocation wall configurations found in fatigue testing. Numerical results for equilibrium distributions of collections of dislocations in doubly periodic arrays of cells, which showed a strong tendency for sharp dislocation walls to form, were presented by Lubarda *et al.* (1993). The importance of a small disorder and the end effects on the elastic fields of nearly periodic dislocation walls was examined by Saada and Bouchaud (1993). Among other uses, a study of the stress field due to dislocation walls or grain boundaries is needed to determine the forces exerted by the grain boundaries. They can pin the approaching dislocations and prevent them to slip through the boundaries, which has a significance in dislocation based analysis of plastic deformation in crystalline solids.

PII S0167-6636(96)00009-9

In this paper we give a simple but systematic analysis of the stress field in infinite and semi-infinite bodies produced by the walls of identical edge dislocations. Finite, infinite, and semi-infinite walls of uniform dislocation spacing are all considered. The results are derived for walls that consist of discrete distribution of dislocations, and are compared with the results obtained for the walls modeled by a continuous distribution of infinitesimal dislocations. Sufficiently away from the dislocation cores of a discrete wall, the stresses coincide with those of a continuous wall. The stress relaxation effects due to the presence of free surface are illustrated by considering finite and infinite walls near the boundary of a semi-infinite body. The long range stresses are exerted by finite walls or tilt segments in both infinite and semi-infinite bodies. A stress divergence, or its absence, is then discussed for various wall configurations. It is shown that normal stresses due to continuous semi-infinite wall in an infinite body diverge everywhere, while divergence in a semi-infinite body occurs only at the location of the leading dislocation in the wall. Some relevant problems left for further study are also indicated. The stress fields due to dislocation walls at the interface between two different materials are presented in the accompanying paper (Lubarda and Kouris, 1996).

2. Dislocation walls in an infinite body

2.1. Dislocation walls with discrete dislocation distribution

Consider a dislocation wall in an infinite elastic body consisting of identical, uniformly spaced edge dislocations along the y axis, from $y = L_1$ to $y = L_2$ (Fig. 1). Let $L_1 = N_1 h$ and $L_2 = N_2 h$, where h is the uniform dislocation spacing, so that the wall consists of $N_2 - N_1 + 1$ dislocations. The in-plane stresses at an arbitrary point (x, y) are obtained by adding the contributions from all dislocations in the wall. Using the well-known

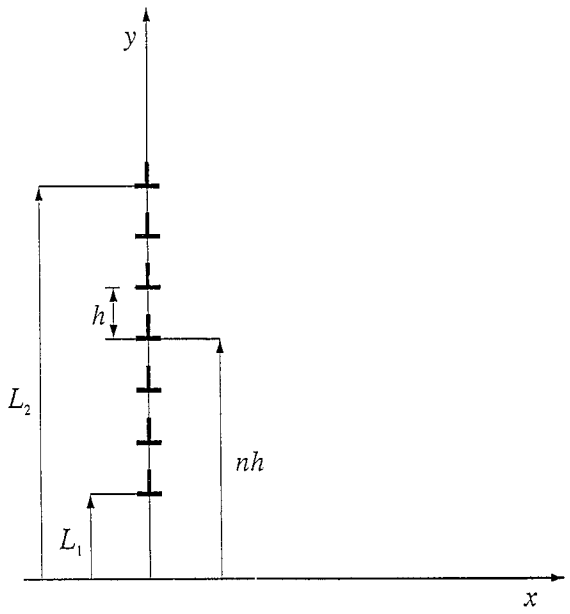

Fig. 1. A finite dislocation wall of identical edge dislocation with spacing h, along the y-axis from L_1 to L_2.

expressions for the stresses due to a single dislocation at the point (0, nh) (Hirth and Lothe (1968), p. 74), one obtains the stresses for the dislocation wall

$$\sigma_x = -k_0 b \sum_{n=N_1}^{N_2} \frac{(y-nh)\left[3x^2+(y-nh)^2\right]}{\left[x^2+(y-nh)^2\right]^2} \tag{1}$$

$$\sigma_y = k_0 b \sum_{n=N_1}^{N_2} \frac{(y-nh)\left[x^2-(y-nh)^2\right]}{\left[x^2+(y-nh)^2\right]^2} \tag{2}$$

$$\tau_{xy} = k_0 b \sum_{n=N_1}^{N_2} \frac{x\left[x^2-(y-nh)^2\right]}{\left[x^2+(y-nh)^2\right]^2}. \tag{3}$$

In Eqs. (1)–(3), b is the magnitude of the Burgers vector, and $k_0 = \mu/2\pi(1-\nu)$, where μ is the shear modulus and ν is the Poisson ratio of the isotropic elastic body.

2.1.1. Infinite wall

If $N_1 = -\infty$ and $N_2 = \infty$, an infinitely long wall in both directions is obtained. The sums appearing in Eqs. (1)–(3) can be performed analytically (Hirth and Lothe (1968), p. 670) yielding

$$\sigma_x = -k\pi \frac{\sin(2\pi\eta)}{A^2}\left[A + 2\pi\xi \sinh(2\pi\xi)\right] \tag{4}$$

$$\sigma_y = -k\pi \frac{\sin(2\pi\eta)}{A^2}\left[A - 2\pi\xi \sinh(2\pi\xi)\right] \tag{5}$$

$$\tau_{xy} = k\pi \frac{2\pi\xi}{A^2}\left[\cosh(2\pi\xi)\cos(2\pi\eta) - 1\right], \tag{6}$$

where $k = k_0 b/h$, and $A = \cosh(2\pi\xi) - \cos(2\pi\eta)$. The non-dimensional variables $\xi = x/h$ and $\eta = y/h$ are conveniently employed. The three stress components are periodic functions of the coordinate η, with a period equal to one, so that along the slip plane of any dislocation in the wall $\sigma_x = \sigma_y = 0$, and $\tau_{xy} = k\pi^2\xi/\sinh^2(\pi\xi)$. The shear stress quickly diminishes away from the wall, and is virtually zero beyond the horizontal distance $2h$ from the wall, where it has already decreased to the value of $0.275 \times 10^{-3} k$.

2.1.2. Semi-infinite wall

A semi-infinite wall in Fig. 2(a) is obtained if $N_1 = 0$ and $N_2 = \infty$. The sums appearing in the expressions for the normal stresses σ_x and σ_y diverge. The sum appearing in the expression for the shear stress converges. It can be easily shown that the shear stress along the slip plane of the leading dislocation in the wall is

$$\tau_{xy} = k\left[\frac{1}{2\xi} + \frac{\pi}{2}\frac{\pi\xi}{\sinh^2(\pi\xi)}\right], \tag{7}$$

while the shear stress along the line parallel to x-axis, at distance Nh from it, is given by

$$\tau_{xy} = k\left\{\frac{\pi}{2}\frac{\pi\xi}{\sinh^2(\pi\xi)} \pm \left[\frac{1}{2\xi} + \xi\sum_{n=1}^{M}\frac{\xi^2-n^2}{(\xi^2+n^2)^2}\right]\right\}. \tag{8}$$

In Eq. (8), the plus sign applies with $M = N$ if the line is above the x-axis, while the minus sign and $M = N-1$ apply if the line is below the x-axis (Fig. 2a). The plots of the shear stress along these two lines and

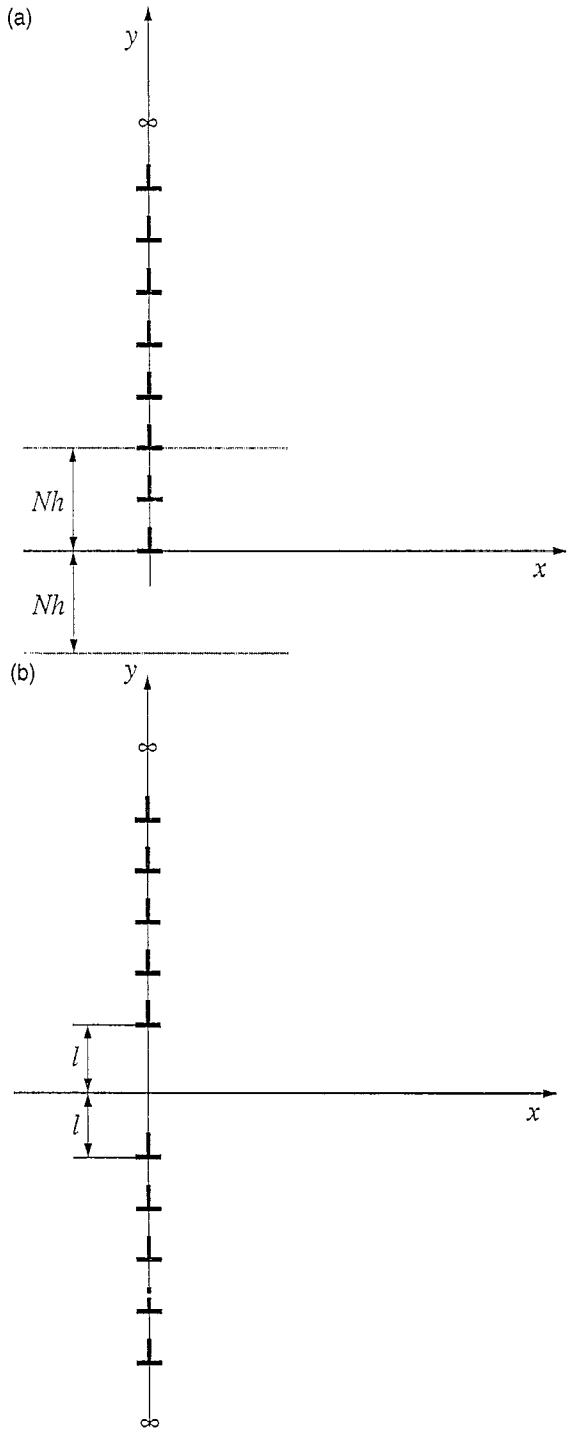

Fig. 2. (a) A semi-infinite wall along the positive y-axis. The dotted lines indicate two slip planes at distance Nh above and below the leading dislocation of the wall. (b) Two identical semi-infinite dislocation walls with the distance $2l$ between their leading dislocations.

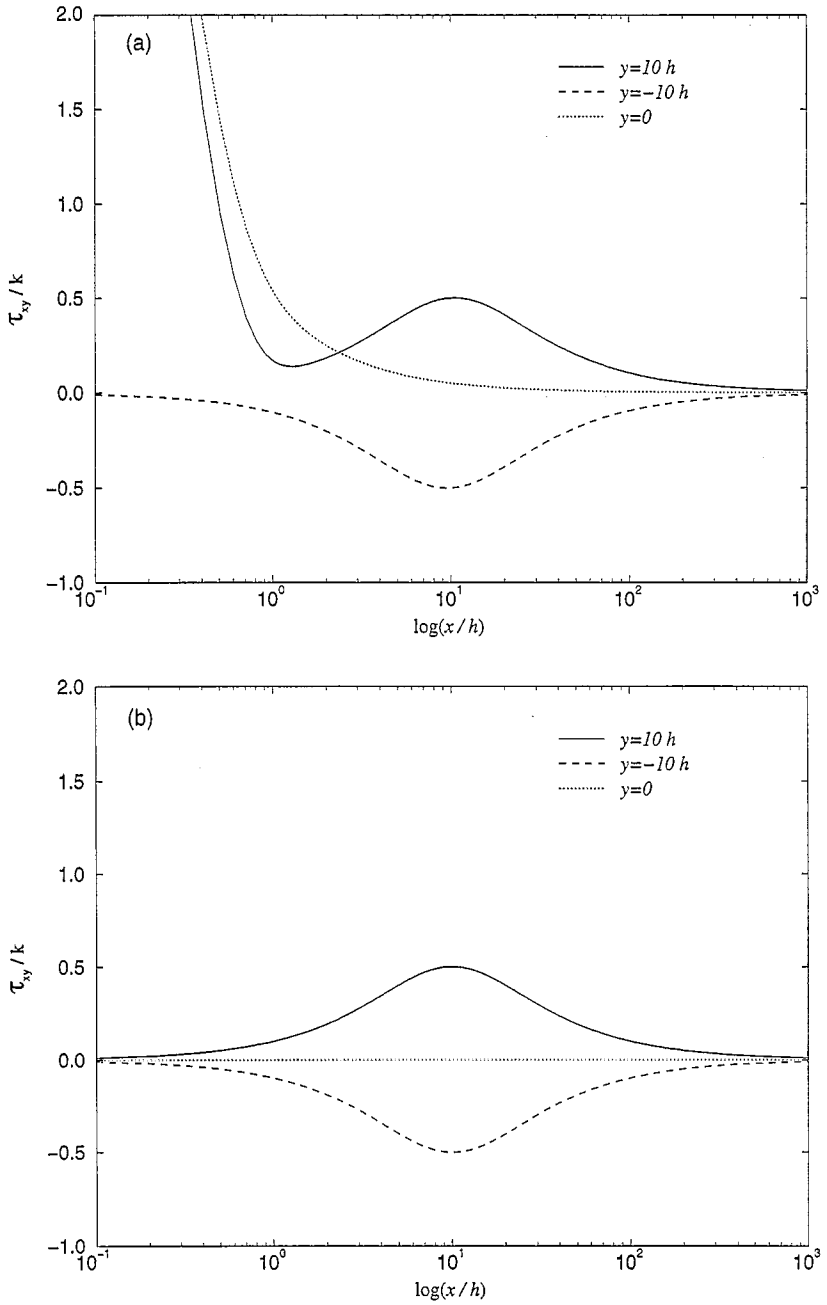

Fig. 3. The shear stress variation due to semi-infinite wall from Fig. 2a, along the x-axis, at distance $\pm 10h$ from it: (a) discrete dislocation distribution; (b) continuous dislocation distribution.

along the x-axis, in the case $N = 10$, are shown in Fig. 3(a). The stress diverges at $x = 0$ for the slip planes $y = 0$ and $y = Nh$, due to dislocation cores there. No divergence occurs along the slip plane $y = -Nh$, where the shear stress is opposite in sign, but otherwise identical to that along the slip plane $y = Nh$, away from the dislocation wall.

If there are two semi-infinite walls, with the same uniform dislocation spacing and with the same Burgers vector, positioned one above another along the y-axis at distance $2l$ (Fig. 2b), all stresses become finite everywhere, except at the core of each dislocation. This is so because this wall structure can be considered to be a superposition of an infinite dislocation wall, and a finite wall of length $2l$ containing dislocations of the opposite sign. Both of these walls give rise to finite stresses everywhere away from the dislocation cores.

2.1.3. Finite wall

The stresses produced by a finite wall of length $2l = 2Nh$, with $2N + 1$ dislocations, symmetrically positioned with respect to the x-axis, are obtained from Eqs. (1)–(3) by using $N_1 = -N$ and $N_2 = N$. The plot of the shear stress along the x-axis for the wall of 101 dislocations is shown in Fig. 4(a). It is noted that a possible disturbance in uniform dislocation spacing near the ends of the wall, due to large climb force there tending to push the leading dislocations out of the wall, has not been here considered. If x is close to the wall, the solid curve in Fig. 4(a) essentially coincides with that obtained for an infinite wall. As discussed by Lubarda et al. (1993), the behavior dramatically changes further away from the wall, where the shear stress starts building up to reach its local maximum of k at the horizontal distance $50.5h$ from the wall. The shear stress than decays and approaches zero asymptotically at large x. The same features are exhibited by any finite wall. For example, for the wall of 10,001 dislocations, a stress bump is shifted further away from the wall, reaching the same maximum value of k, at the distance $5{,}000h$ from the wall (half the wall length). This illustrates the long range stress effect exerted by finite or bounded wall. Other dislocation structures may also exert a long range stress effect. For example, Hirth and Lothe (1968) give an example of an infinite dislocation array that consists of identical edge dislocations of uniform spacing all lying along the same slip plane (say, x-axis), which exerts a non-vanishing normal stress σ_x as $y \to \pm\infty$.

The variation of the shear stress in Fig. 4(a) is also shown along the several lines parallel to x-axis, i.e., along the slip plane of the bottom dislocation in the wall, and at the distances l and $2l$ below. Fig. 5(a) shows the same in the case of the normal stress σ_x. Due to symmetry of dislocation distribution, the normal stress σ_x is equal to zero along the x-axis.

2.2. Dislocation walls with continuous dislocation distribution

We now consider dislocation walls modeled by a continuous distribution of infinitesimal dislocations with density $1/h$ and, therefore, with the specific Burgers vector of magnitude b/h. For the wall along the y-axis extending from L_1 to L_2, as in Fig. 1, the stresses are obtained by an appropriate integration, which gives

$$\sigma_x = k\left[\frac{1}{2}\ln\frac{x^2+(y-L_2)^2}{x^2+(y-L_1)^2} + \frac{x^2}{x^2+(y-L_1)^2} - \frac{x^2}{x^2+(y-L_2)^2}\right] \tag{9}$$

$$\sigma_y = k\left[\frac{1}{2}\ln\frac{x^2+(y-L_2)^2}{x^2+(y-L_1)^2} - \frac{x^2}{x^2+(y-L_1)^2} + \frac{x^2}{x^2+(y-L_2)^2}\right] \tag{10}$$

$$\tau_{xy} = kx\left[\frac{y-L_1}{x^2+(y-L_1)^2} - \frac{y-L_2}{x^2+(y-L_2)^2}\right]. \tag{11}$$

2.2.1. Infinite wall

An infinite wall of continuously distributed dislocations is obtained if $L_1 = -\infty$ and $L_2 = \infty$. In this case from Eqs. (9)–(11) follows that all stress components vanish, i.e., $\sigma_x = \sigma_y = \tau_{xy} = 0$. The existence of a narrow longitudinal layer around the wall with the significant stresses in the case of a discrete dislocation distribution is, therefore, lost when the wall is modeled by a continuous distribution of infinitesimal dislocations. The physical

consequence of the presence of an infinite dislocation wall in an infinite body is the relative rotation (b/h) of the (structural) orientation of two halves of the infinite body, of the type caused in crystals by a tilt boundary (Gilman (1969), p. 118). This can be observed by considering an infinite dislocation wall as a disclination dipole along the y-axis, with the center at $x = 0$.

2.2.2. Semi-infinite wall

If $L_1 = 0$ and $L_2 = \infty$ are substituted in Eqs. (9)–(11), the stress distribution for a semi-infinite wall is obtained. In this case both normal stresses diverge, while the shear stress becomes

$$\tau_{xy} = k\frac{xy}{x^2 + y^2}, \tag{12}$$

as given by Hirth and Lothe (1968), p. 711. This shear stress distribution is antisymmetric with respect to the x-axis. The plots along the lines $y = \pm 10h$ are shown in Fig. 3(b). These plots parallel the plots in Fig. 3(a), corresponding to discrete distributions of dislocations in a semi-infinite wall. Note that the maximum value of τ_{xy} along any line parallel to the x-axis is the same and equal to $k/2$. The location of this maximum along the horizontal axis is exactly equal to the distance between the leading dislocation in the wall and the considered horizontal axis (i.e., at $x = 10h$ in the case of Fig. 3b). There is no singularity of shear stress along the wall of continuously distributed infinitesimal dislocations, except at the place of the leading dislocation in the wall. Although both normal stresses σ_x and σ_y diverge, from Eqs. (12) and (13) it follows that the stress difference $\sigma_x - \sigma_y$ is finite and equal to $2kx^2/(x^2 + y^2)$. Hence, the shear stress over any plane in the body is also finite. If two identical semi-infinite walls are along the y-axis vertically apart by $2l$, the divergent terms in the expressions for the normal stresses σ_x and σ_y due to individual walls cancel each other, and all stress components become finite everywhere, except at the location of the leading dislocation in each wall $(y = \pm l)$. By employing Eqs. (9)–(11), the stress components are derived as

$$\sigma_x = k\left[\frac{1}{2}\ln\frac{x^2 + (y+l)^2}{x^2 + (y-l)^2} + \frac{x^2}{x^2 + (y-l)^2} - \frac{x^2}{x^2 + (y+l)^2}\right] \tag{13}$$

$$\sigma_y = k\left[\frac{1}{2}\ln\frac{x^2 + (y+l)^2}{x^2 + (y-l)^2} - \frac{x^2}{x^2 + (y-l)^2} + \frac{x^2}{x^2 + (y+l)^2}\right] \tag{14}$$

$$\tau_{xy} = kx\left[\frac{y-l}{x^2 + (y-l)^2} - \frac{y+l}{x^2 + (y+l)^2}\right]. \tag{15}$$

These expressions coincide with those of a disclination dipole, given by Li (1972), who derived them by superimposing stress fields of two wedge dislocations, derived by Huang and Mura (1970). They are used later in the paper to derive the stress distribution due to a dislocation wall in a semi-infinite body. See also deWit (1973).

2.2.3. Finite wall

The stresses produced by a finite dislocation wall of length $2l$, symmetrically positioned with respect to the x-axis, are obtained from Eqs. (9)–(11) by substituting $L_1 = -l$ and $L_2 = l$. Along the x-axis normal stresses are zero, while the plot of shear stress for the wall of length $2l = 100h$ is shown by a solid curve in Fig. 4b. It is interesting to observe that this shear stress is exactly twice as large as the shear stress along the line at distance l above the leading dislocation of a semi-infinite continuous dislocation wall. Again, in contrast to walls with a

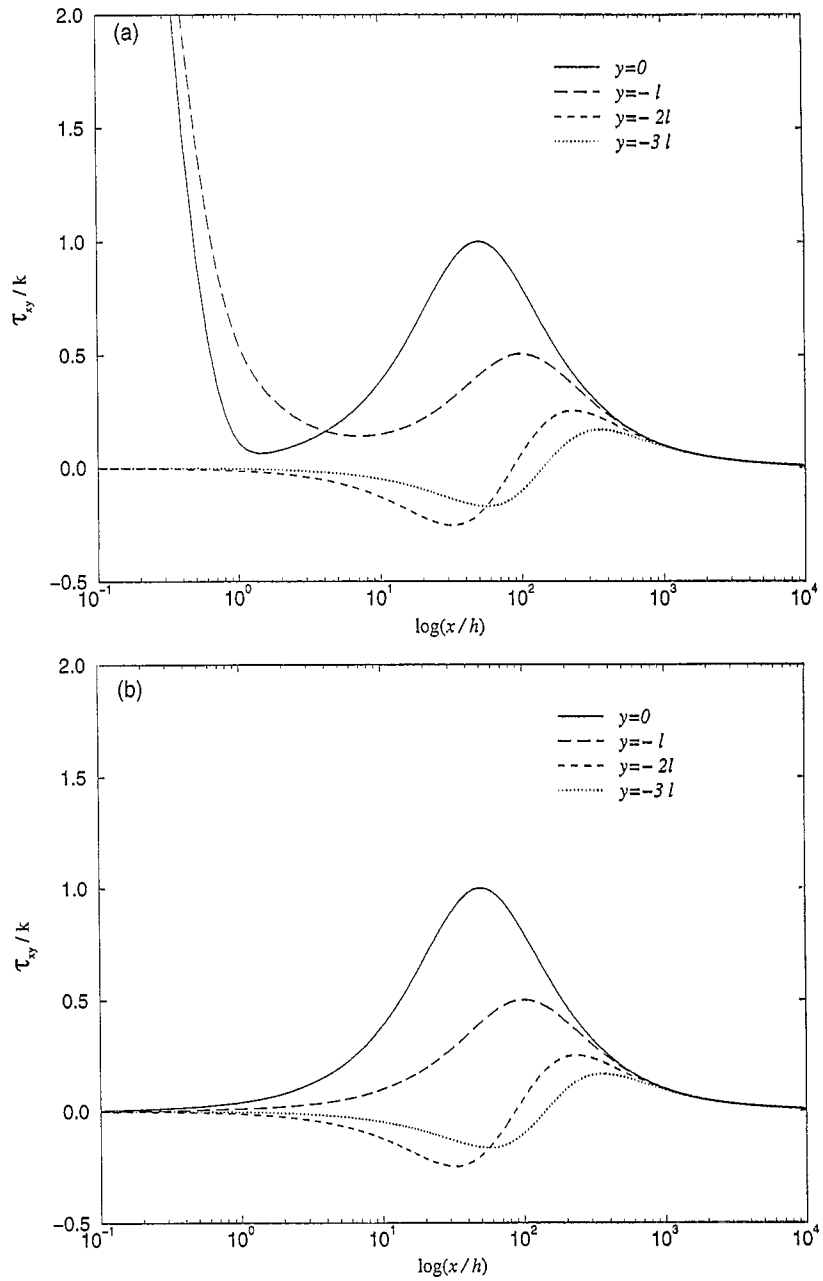

Fig. 4. The shear stress variation due to finite wall of 101 dislocations in an infinite body, along the x-axis through the middle of the wall and several parallel lines: (a) discrete dislocation distribution; (b) continuous dislocation distribution.

discrete dislocation distribution, there is no singularity in stress at $x = 0$. Fig. 4b also shows the variation of shear stress along three lines parallel to x-axis, at distances l, $2l$ and $3l$ below the center of the wall of length $2l$. The normal stress σ_x along these lines is shown in Fig. 5(b). This should be compared with plots in Figs.

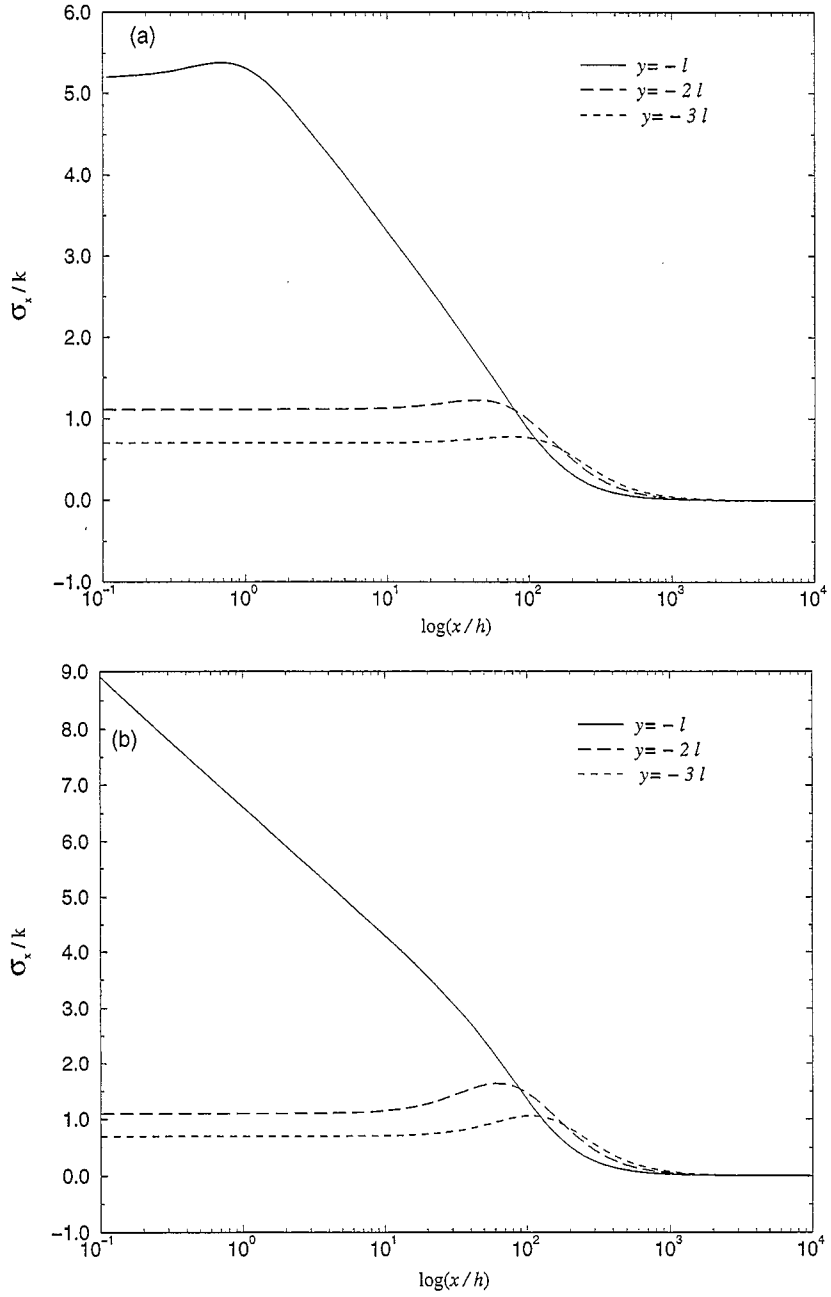

Fig. 5. The normal stress variation σ_x due to finite wall of 101 dislocations in an infinite body, along several parallel lines below the middle of the wall: (a) discrete dislocation distribution; (b) continuous dislocation distribution.

4(a) and 5(a), corresponding to discrete dislocation distribution. As expected, the stresses tend to coincide away from any dislocation in a discrete wall. At the locations of the end dislocations in a continuous wall, the normal stress diverges logarithmically, and on the log scale the stress changes linearly along the horizontal line near the wall (Fig. 5b).

3. Dislocation walls in a semi-infinite body

3.1. Dislocation walls with discrete dislocation distribution

Consider a dislocation wall consisting of $2N + 1$ dislocations with uniform spacing h, at distance l from the free surface in a semi-infinite body (Fig. 6b). The length of the wall is $L = 2Nh$. Let $l = mh$, for some integer

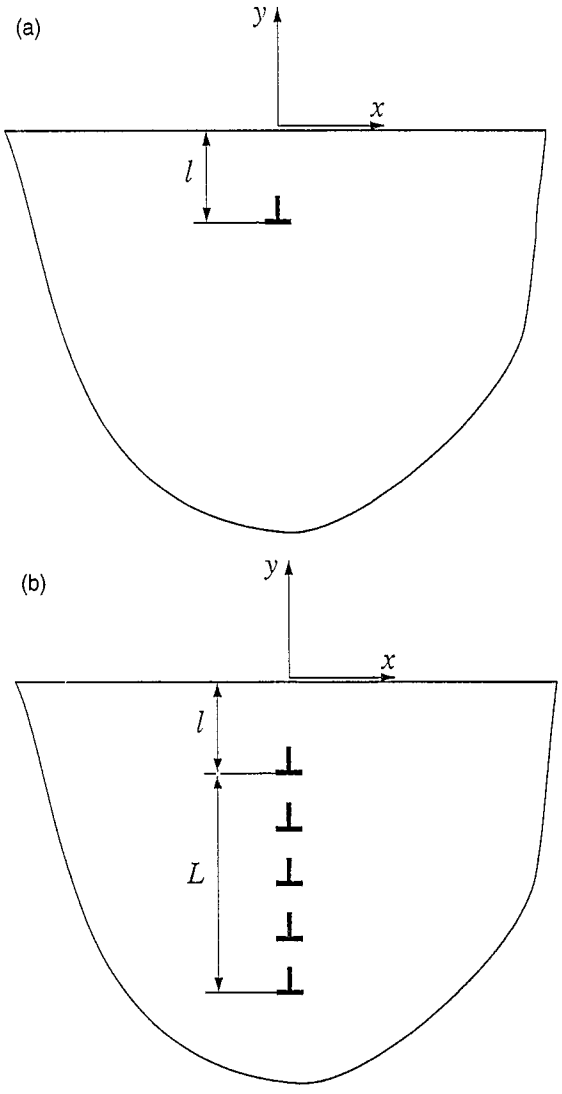

Fig. 6. (a) An edge dislocation in a semi-infinite body at distance l from its free surface. The dislocation Burgers vector is parallel to free surface; (b) A dislocation wall of length L in a semi-infinite body at distance l between the leading dislocation in the wall and the free surface.

m. The stresses produced by this wall are obtained by summing the stresses derived in the Appendix A for a single dislocation in a semi-infinite body, i.e. Eqs. (A.1)–(A.3) and Eqs. (A.8)–(A.10), which gives

$$\sigma_x = -k_0 b \sum_{n=m}^{2N+m} \left\{ \frac{(y+nh)\left[3x^2+(y+nh)^2\right]}{\left[x^2+(y+nh)^2\right]^2} - \frac{(y-nh)\left[3x^2+(y-nh)^2\right]}{\left[x^2+(y-nh)^2\right]^2} \right.$$

$$\left. -2nh\frac{(y-nh)^4-2y(y-nh)^3+6x^2y(y-nh)-x^4}{\left[x^2+(y-nh)^2\right]^3} \right\} \tag{16}$$

$$\sigma_y = k_0 b \sum_{n=m}^{2N+m} \left\{ \frac{(y+nh)\left[x^2-(y+nh)^2\right]}{\left[x^2+(y+nh)^2\right]^2} - \frac{(y-nh)\left[x^2-(y-nh)^2\right]}{\left[x^2+(y-nh)^2\right]^2} \right.$$

$$\left. +2nh\frac{(y-nh)^4+2y(y-nh)^3-6x^2y(y-nh)-x^4}{\left[x^2+(y-nh)^2\right]^3} \right\} \tag{17}$$

$$\tau_{xy} = k_0 b \sum_{n=m}^{2N+m} \left\{ \frac{x\left[x^2-(y+nh)^2\right]}{\left[x^2+(y+nh)^2\right]^2} - \frac{x\left[x^2-(y-nh)^2\right]}{\left[x^2+(y-nh)^2\right]^2} + 4nh\frac{xy\left[3(y-nh)^2-x^2\right]}{\left[x^2+(y-nh)^2\right]^3} \right\}. \tag{18}$$

3.1.1. Semi-infinite wall

A semi-infinite wall with the leading dislocation of the wall at distance l from the free surface is obtained if $N \to \infty$. The divergent parts of the sums (of the type, sum of $1/n$ with n going from one to infinity), appearing in the expressions (16) and (17) for the normal stresses σ_x and σ_y, cancel each other and stresses become finite everywhere, except at the core centers of the individual dislocations in the wall. This is in contrast to the situation with a semi-infinite wall in an infinite medium, where normal stresses are everywhere divergent.

Since it is difficult to obtain a closed form analytical solution for the sums in (16)–(18), to illustrate the stress variation due to semi-infinite wall, consider the wall containing 10,001 dislocations, at distance $l = 10h$ from the boundary. The shear stress variations along the lines parallel to the boundary, and at distances $l/2$, l, and $2l$ below, are shown in Fig. 7(a). Along these lines the other end of the wall (about $1000l$ away) is not observed, and the wall acts as a semi-infinite wall. Only at horizontal distance greater than about $100l$ from the wall, the other end of the wall becomes recognized, and the stress tends to reappear, albeit with a very small (negligible) magnitude. Further down the wall, the lower end of the wall becomes more evident, and the wall acts as a finite wall in a semi-infinite body. For example, the shear stress along the line $100l$ below the free surface is shown by a dashed curve in Fig. 8. Initially, the wall behaves as a semi-infinite, but at large horizontal distances away from the wall, the wall acts as a finite wall. The stress bump appears, with a maximum stress of $0.2245k$, at the horizontal distance of about $600l$ from the wall. This again illustrates the long range effect of a finite dislocation wall, this time in a semi-infinite body. For comparison, the shear stress along the same horizontal line relative to the wall in an infinite body is shown by a solid curve in Fig. 8. The maximum stress in the bump is now equal to $0.6235k$, and occurs at distances of about $135l$ and $670l$ from the wall. The presence of a free surface in this case, therefore, relaxes the magnitude of the maximum shear stress, and the extent of the

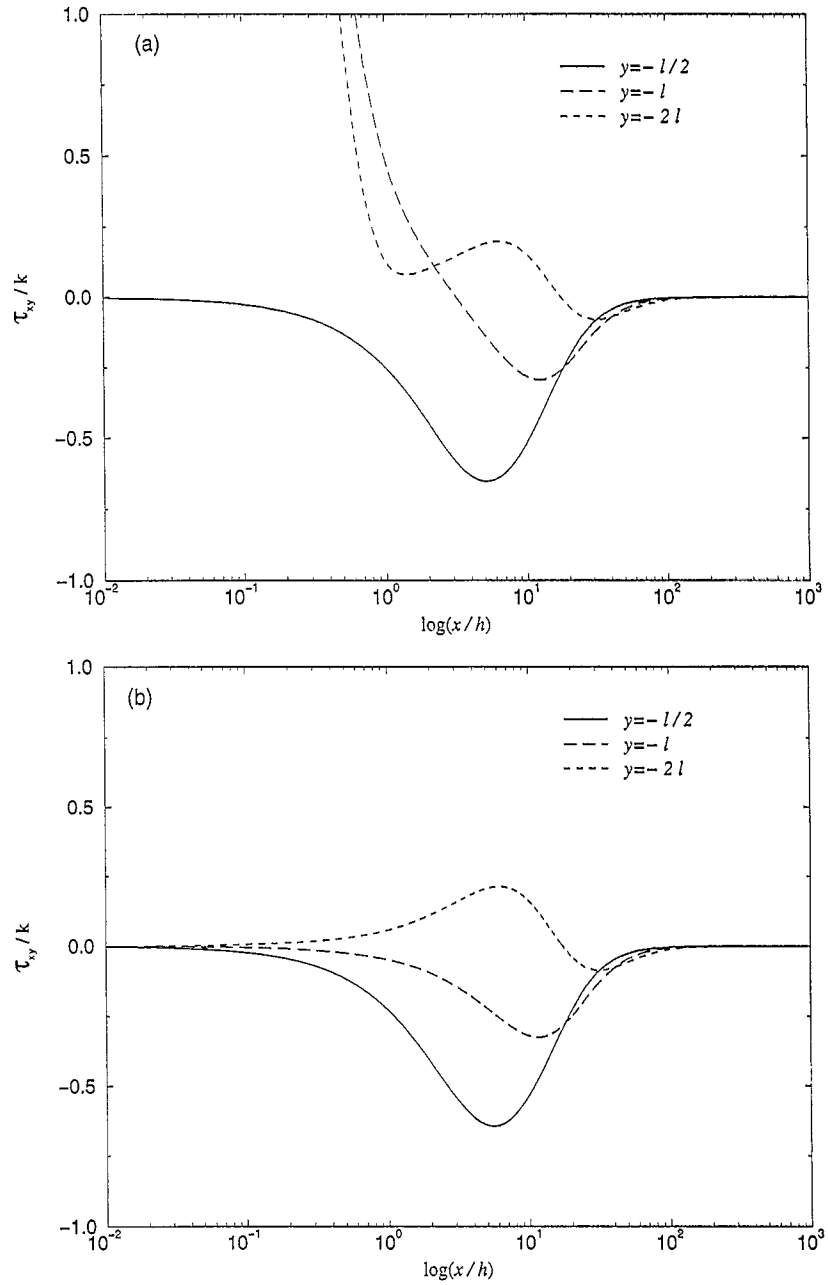

Fig. 7. The shear stress variation in a semi-infinite body due to semi-infinite dislocation wall at distance l between the leading dislocation in the wall and the free surface ($y = 0$): (a) discrete dislocation distribution; (b) continuous dislocation distribution.

significant long range stress effect. Recall that the maximum shear stress in the bump along the horizontal line that intersects the wall at the middle of its hight is equal to k, and occurs at distance $500l$ away from the wall of length $1000l$.

3.1.2. Finite wall

Consider a finite wall of length $L = 10l$, at distance $l = 10h$ below the free surface. Fig. 10(a) shows the shear stress behavior obtained from Eq. (18) along the lines parallel to the free surface, at distances $l/2$, l, $l + L/2$, $l + L$, and $l + 3L/2$ below. These plots should be compared to plots in Fig. 4(a), corresponding to finite wall in an infinite body. To illustrate the effect of the free surface on the stress distribution due to finite wall, consider the variation of the shear stress along the horizontal line at the middle of the wall. When the wall of 101 dislocations is in an infinite body, the local maximum of the shear stress is k and occurs at distance $50.5h$ from the wall (Fig. 4a). In the case of the same wall in a semi-infinite body, at distance $l = 10h$ below the free surface, the local shear stress maximum is $0.658k$ and occurs at the distance $53.1h$ from the wall (Fig. 10a). Finally, it should be mentioned that along the lines at large distances under the wall, the stress behavior approaches that due to a single dislocation of the magnified Burgers vector $(2N + 1)b$ located at the center of the wall, i.e., at distance $l + L/2$ below the free surface.

3.2. Dislocation walls with continuous dislocation distribution

When a dislocation wall is modeled by a continuous dislocation distribution, the Airy stress function corresponding to wall of length L, at distance l from the free surface, is found by integrating expression (A.12) for the Airy stress function of a single dislocation, i.e.

$$\Phi = k\int_{l}^{L+l}\left[\frac{1}{2}(y+v)\ln\frac{x^2+(y-v)^2}{x^2+(y+v)^2} - 2v\frac{y(y-v)}{x^2+(y-v)^2}\right]\mathrm{d}v. \tag{19}$$

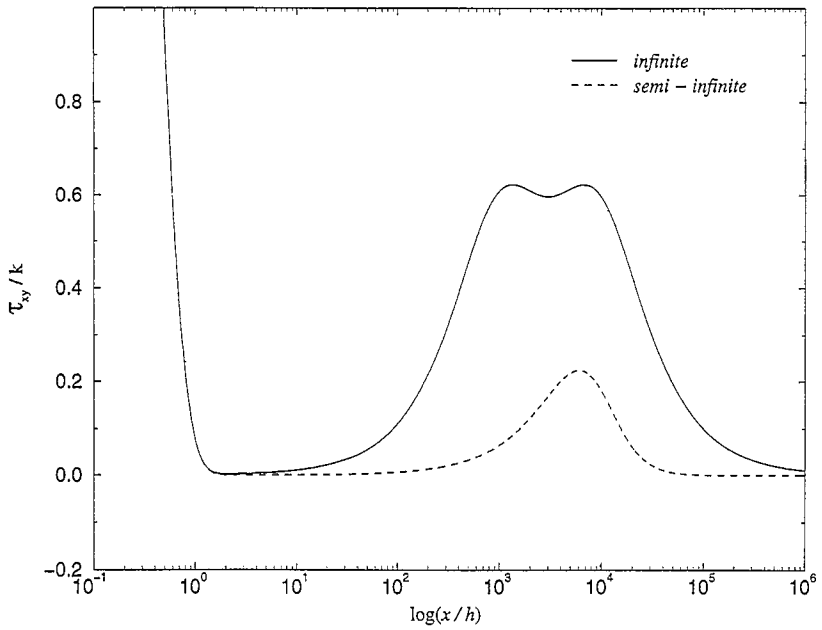

Fig. 8. A long range shear stress effect due to finite wall of 10,001 dislocations of uniform spacing h. The dashed curve corresponds to the wall in a semi-infinite body, when the leading dislocation of the wall is at distance $l = 10h$ below the free surface. The stress is plotted along the horizontal line at distance $100l$ below the free surface. The solid curve gives the shear stress along the same horizontal line relative to the wall, when the wall is in an infinite body.

This gives

$$\Phi = \frac{k}{4}\left\{\left[x^2+(y+v)^2\right]\ln\frac{x^2+(y-v)^2}{x^2+(y+v)^2}\right\}_{\Delta}. \tag{20}$$

The symbolic notation $\}_{\Delta}$ indicates that the expression within the brackets is evaluated at $v=l$, and the result subtracted from that obtained at $v=L+l$. It should be pointed out that Eshelby (1966) has shown that the elastic field of an edge dislocation can be obtained from that of a wedge dislocation (or disclination) simply by differentiation. In Eq. (19) an inverse property was essentially used, by which the Airy stress function of a disclination (which is equivalent to a semi-infinite continuous wall of infinitesimal dislocations), follows by integration from the Airy stress function corresponding to a single dislocation.
The stresses are obtained from (20) by differentiation, and are given by

$$\sigma_x = \frac{k}{2}\left\{-\mathscr{L}(x,y,v)+4v\frac{(y-2v)\left[(y^2-v^2)^2+x^2(x^2+2v^2)\right]-2x^2y^2(y+2v)}{\left[x^2+(y-v)^2\right]^2\left[x^2+(y+v)^2\right]}\right\}_{\Delta} \tag{21}$$

$$\sigma_y = \frac{k}{2}\left\{-\mathscr{L}(x,y,v)+4vy\frac{(y^2-v^2)^2+x^2(x^2+2y^2-8vy+2v^2)}{\left[x^2+(y-v)^2\right]^2\left[x^2+(y+v)^2\right]}\right\}_{\Delta} \tag{22}$$

$$\tau_{xy} = 8k\left\{v^2xy\frac{y^2-x^2-v^2}{\left[x^2+(y-v)^2\right]^2\left[x^2+(y+v)^2\right]}\right\}_{\Delta}, \tag{23}$$

where

$$\mathscr{L}(x,y,v) = \ln\frac{x^2+(y+v)^2}{x^2+(y-v)^2}. \tag{24}$$

The expressions (21)–(23) can be alternatively obtained by integrating the stress components corresponding to a single dislocation in a semi-infinite body, i.e., the sums of the appropriate expressions from (A.1)–(A.3), and (A.8)–(A.10). Yet another derivation is presented in the Appendix B of the paper. Observe from (21) and (22) that normal stresses diverge at the locations of the end dislocations in the wall (i.e., at $y=-l$ and $y=-l-L$).

3.2.1. Semi-infinite wall

A semi-infinite wall at distance l from the free surface is obtained when $L\to\infty$. The expressions (21)–(23) in this case simplify to

$$\sigma_x = \frac{k}{2}\left\{\mathscr{L}(x,y,l)-4l\frac{(y-2l)\left[(y^2-l^2)^2+x^2(x^2+2l^2)\right]-2x^2y^2(y+2l)}{\left[x^2+(y-l)^2\right]^2\left[x^2+(y+l)^2\right]}\right\} \tag{25}$$

$$\sigma_y = \frac{k}{2}\left\{\mathscr{L}(x,y,l)-4ly\frac{(y^2-l^2)^2+x^2(x^2+2y^2-8ly+2l^2)}{\left[x^2+(y-l)^2\right]^2\left[x^2+(y+l)^2\right]}\right\} \tag{26}$$

$$\tau_{xy} = 8kl^2xy\frac{x^2-y^2+l^2}{\left[x^2+(y-l)^2\right]^2\left[x^2+(y+l)^2\right]}. \tag{27}$$

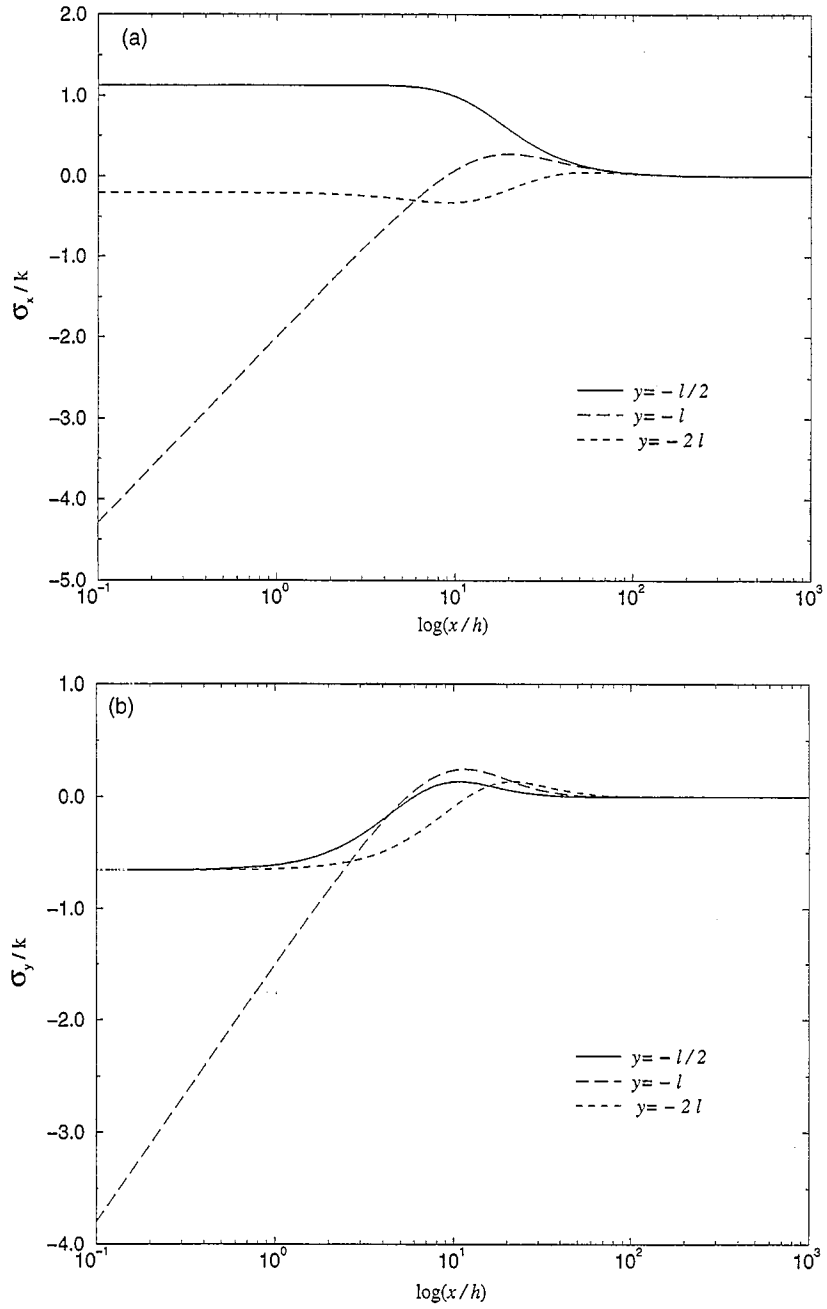

Fig. 9. The normal stress variation in a semi-infinite body due to semi-infinite continuous dislocation wall at distance l between the leading dislocation in the wall and the free surface ($y = 0$): (a) normal stress σ_x; (b) normal stress σ_y.

The shear stress variations for a semi-infinite wall at distance $l = 10h$ from the free surface, along the lines parallel to the boundary and at distances $l/2$, l, and $2l$ below, are shown in Fig. 7(b). The diagrams of normal stresses σ_x and σ_y are shown in Fig. 9. Further down the wall, the stresses quickly diminish and at distance $10l$ below the free surface become almost zero (the maximum shear stress being equal to $0.015k$). To compare the plots with those corresponding to discrete dislocation distribution in the wall, consider the shear stress variation.

Above the leading dislocation in the wall, i.e., at distance $l/2$ from the free surface, the solutions for the discrete and continuous walls essentially coincide all along the horizontal line. They also coincide away from the wall along the horizontal lines intersecting the walls. Near the wall, however, the shear stress corresponding to discrete dislocation distribution increases indefinitely as the dislocation core center is approached, while the shear stress vanishes there in the case of the wall with a continuous distribution of infinitesimal dislocations. Recall also that in the case of a continuous semi-infinite dislocation wall in an infinite body (Fig. 3b), the magnitude of the maximum shear stress is equal to $k/2$ along any horizontal line not passing through the leading dislocation of the wall.

Note from (25)–(27) that all three stress components are finite everywhere in the semi-infinite body, except at the location of the leading dislocation in the wall ($x = 0$, $y = -l$), where the normal stresses σ_x and σ_y become infinite. Consequently, the climb force per unit length of a dislocation ($\sigma_x b$) is very large at the top of the semi-infinite wall, tending to push leading dislocation and disturb uniform dislocation spacing near the end of the wall. It is also observed from (25)–(27) that all stresses vanish for $l = 0$. In this case the dislocation wall completely separates two parts of the semi-infinite body, causing them to rotate relative to each other.

3.2.2. Finite wall

Fig. 10(b) shows the shear stress behavior obtained from Eq. (27) in the case of a finite continuous wall of length $L = 10l$, at distance $l = 10h$ below the free surface. The variations are plotted along the lines $y = -l/2$, $-l$, $-(l + L/2)$, $-(l + L)$, and $-(l + 3L/2)$, to compare them with the corresponding behavior in the case of discrete walls, shown in Fig. 10(a). The plots are self-explanatory. Finally, Fig. 11 gives the normal stress variation due to the considered finite wall. Observe the logarithmic divergence in both normal stress components near the wall, along the slip planes passing through the end dislocations of the continuous wall.

4. Conclusion

An analysis of the stress fields produced by walls of identical edge dislocations in infinite and semi-infinite bodies is given in this paper. Finite, infinite, and semi-infinite walls of uniform dislocation spacing are considered. The walls with discrete distribution of dislocations, as well as with a continuous distribution of infinitesimal dislocations, are considered in detail. Sufficiently away from the dislocation cores of a discrete wall, the stresses coincide with those of a continuous wall. The effects of the free surface on the stress distribution are illustrated for finite and infinite walls near the boundary of a semi-infinite body. The presence of the free surface usually relaxes the stresses obtained for the wall in an infinite medium. It is further shown that a long range stress is exerted by bounded walls in both infinite and semi-infinite bodies. The question of divergence of the stress field is then discussed for various wall configurations. For example, it is shown that the normal stresses due to continuous semi-infinite wall in an infinite body diverge everywhere, while divergence occurs in a semi-infinite body only at the location of the leading dislocation in the wall.

It would be of interest to derive the stress distribution due to dislocation walls in a thin plate or layer. The stress field due to edge dislocation with the Burgers vector parallel to the plate free surfaces has been solved by Nabarro and Kostlan (1978) in a special case when a dislocation is located at the center of the plate thickness. Lee and Dundurs (1973) solved the case of an edge dislocation with its Burgers vector normal to the plate surface. Other available solutions and additional list of references can be found in Gutkin and Romanov (1991). See also Lothe (1992). The stress field due to dislocation walls at the interface between two different materials is presented in the accompanying paper (Lubarda and Kouris, 1996). Further work should also address a determination of the stress field exerted by dislocation walls and other arrays at the interfaces of a multilayer material.

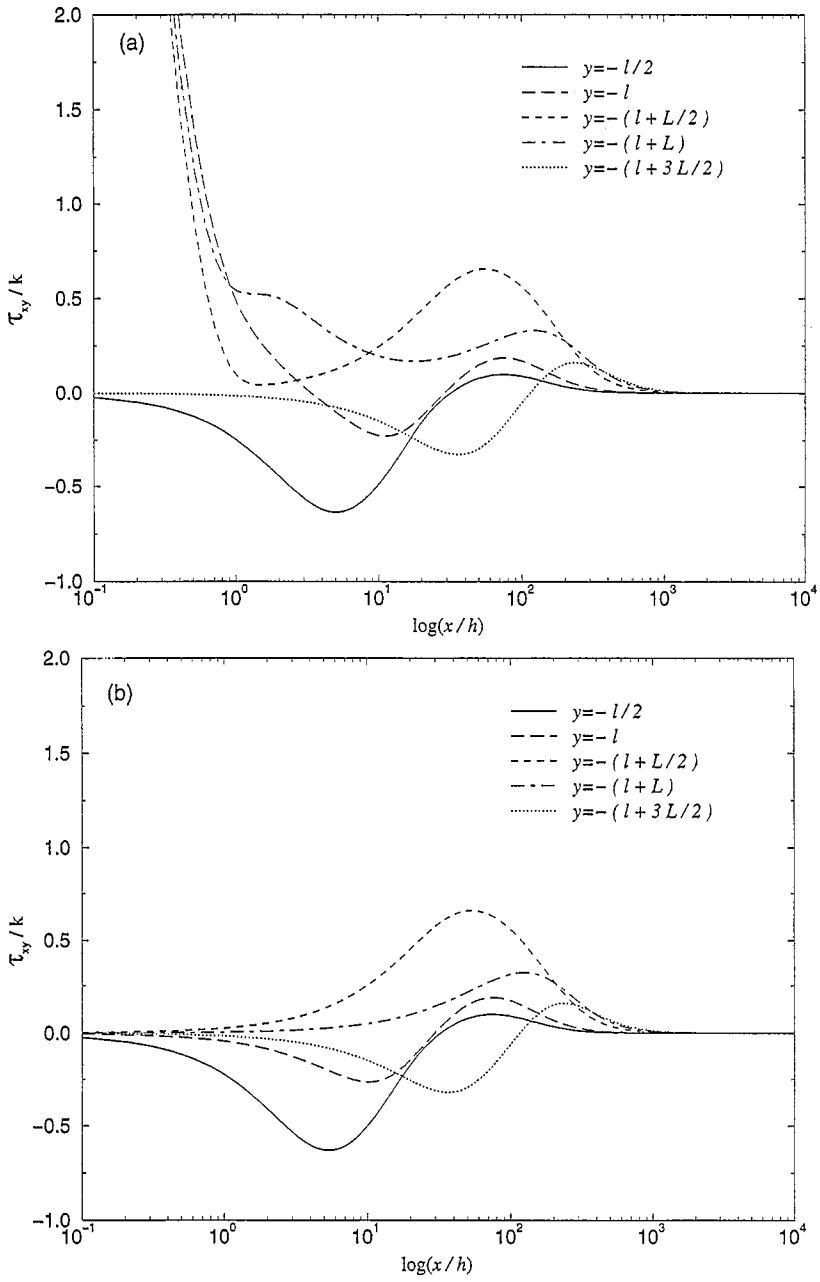

Fig. 10. The shear stress variation in a semi-infinite body due to finite dislocation wall of length $L = 10l$, at distance l between the leading dislocation in the wall and the free surface ($y = 0$): (a) discrete dislocation distribution; (b) continuous dislocation distribution.

Acknowledgments

Discussion with Professor Marc Mignolet is kindly acknowledged. The authors also thank Mr. Jaroslaw Knap for helping with the figures.

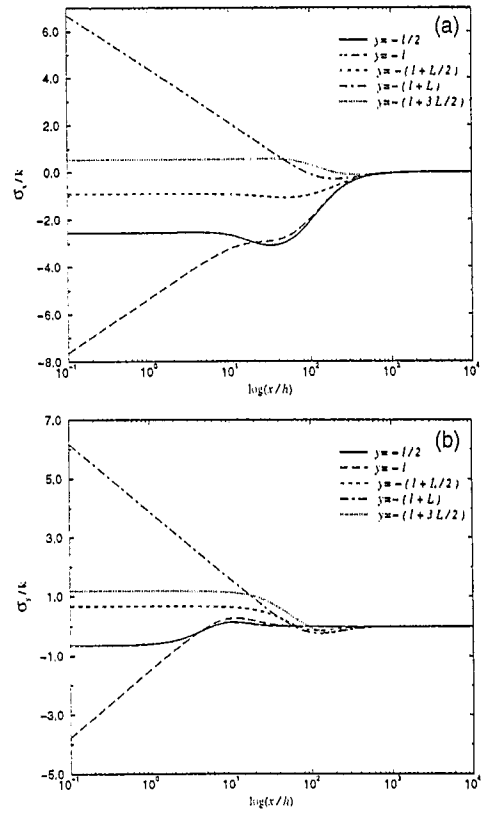

Fig. 11. The normal stress variation in a semi-infinite body due to continuous finite dislocation wall of length $L = 10l$, at distance l between the leading dislocation in the wall and the free surface ($y = 0$): (a) normal stress σ_x; (b) normal stress σ_y.

Appendix A: *Single dislocation near the free surface of a semi-infinite body*

Consider an edge dislocation in a semi-infinite isotropic body at distance l from the free surface, with the Burgers vector parallel to the free surface (Fig. 6a). The stress field caused by this dislocation was originally derived by Head (1953). It can also be derived in an analogous manner to that presented by Hirth and Lothe (1968) for a dislocation with the Burgers vector normal to the free surface. Consider a dislocation in an infinite body at the point $(0, -l)$, and introduce an image dislocation, with the opposite Burgers vector, at the point $(0, l)$. The in-plane stress field due to two dislocations is

$$\sigma_x = -k_0 b\left\{\frac{(y+l)\left[3x^2+(y+l)^2\right]}{\left[x^2+(y+l)^2\right]^2} - \frac{(y-l)\left[3x^2+(y-l)^2\right]}{\left[x^2+(y-l)^2\right]^2}\right\} \tag{A.1}$$

$$\sigma_y = k_0 b\left\{\frac{(y+l)\left[x^2-(y+l)^2\right]}{\left[x^2+(y+l)^2\right]^2} - \frac{(y-l)\left[x^2-(y-l)^2\right]}{\left[x^2+(y-l)^2\right]^2}\right\} \tag{A.2}$$

$$\tau_{xy} = k_0 b\left\{\frac{x\left[x^2-(y+l)^2\right]}{\left[x^2+(y+l)^2\right]^2} - \frac{x\left[x^2-(y-l)^2\right]}{\left[x^2+(y-l)^2\right]^2}\right\}. \tag{A.3}$$

These stresses are associated with the Airy stress function

$$\Phi = -\frac{1}{2}k_0 b\left\{(y+l)\ \ln\left[x^2+(y+l)^2\right]-(y-l)\ \ln\left[x^2+(y-l)^2\right]\right\}, \tag{A.4}$$

through the well-known formulas $\sigma_x = \partial^2\Phi/\partial y^2$, $\sigma_y = \partial^2\Phi/\partial x^2$, and $\tau_{xy} = -\partial^2\Phi/\partial x\partial y$. In order to achieve the stress free surface condition at $y=0$, from (A.2) and (A.3) follows that an additional elastic solution needs to be superimposed, i.e., the stress field in a semi-infinite body produced by the normal stress

$$\sigma_y(x,0) = 2k_0 b\frac{l(l^2-x^2)}{(l^2+x^2)^2}, \tag{A.5}$$

acting over the boundary $y=0$. By employing the symmetry of the stress distribution with respect to y-axis and vanishing behavior of the stress field as $y\to-\infty$, the Airy stress function can be represented by a Fourier integral

$$\Phi = \int_0^\infty c(\alpha)(1-\alpha y)e^{\alpha y}\cos\alpha x\,d\alpha. \tag{A.6}$$

From the boundary condition (A.5) it then follows through a Fourier inversion that $\alpha c(\alpha) = -2k_0 b l e^{-\alpha l}$, and the stress function becomes

$$\Phi = -2k_0 bl\int_0^\infty\left(\frac{1}{\alpha}-y\right)e^{\alpha(y-l)}\cos\alpha x\,d\alpha. \tag{A.7}$$

The integral in (A.7) is a divergent integral due to behavior of the integrant at $\alpha=0$, but its derivatives with respect to x and y are convergent integrals and, therefore, (A.7) can be used to derive the corresponding stress distribution. This gives

$$\sigma_x = 2k_0 bl\frac{(y-l)^4-2y(y-l)^3+6x^2y(y-l)-x^4}{\left[x^2+(y-l)^2\right]^3} \tag{A.8}$$

$$\sigma_y = 2k_0 bl\frac{(y-l)^4+2y(y-l)^3-6x^2y(y-l)-x^4}{\left[x^2+(y-l)^2\right]^3} \tag{A.9}$$

$$\tau_{xy} = 4k_0 bl\frac{xy\left[3(y-l)^2-x^2\right]}{\left[x^2+(y-l)^2\right]^3}. \tag{A.10}$$

The Airy stress function can now be deduced from (A.8)–(A.10) by integration, and is found to be

$$\Phi = 2k_0 bl\left\{\frac{1}{2}\ln\left[x^2+(y-l)^2\right]-\frac{y(y-l)}{x^2+(y-l)^2}\right\}. \tag{A.11}$$

By summing (A.4) and (A.11), the Airy stress function for the stress distribution due to a single dislocation in a semi-infinite body, at distance l from its free surface, is

$$\Phi = k_0 b\left[\frac{1}{2}(y+l)\ \ln\frac{x^2+(y-l)^2}{x^2+(y+l)^2}-2l\frac{y(y-l)}{x^2+(y-l)^2}\right]. \tag{A.12}$$

The total stresses are the sums of the corresponding stress components from (A.1)–(A.3), and (A.8)–(A.10). The above expressions also follow as a special case from the results for the stress field due to an edge dislocation near the interface of two different materials (Head, 1953; Dundurs and Mura, 1964; Dundurs, 1969). See also Lothe (1992), and Belov (1992).

Appendix B: *Dislocation wall near the free surface of a semi-infinite body*

An alternative derivation, to that presented in Section 3.2, of the stress field due to dislocation wall in a semi-infinite body is here presented. Consider two identical continuous semi-infinite dislocation walls in an infinite body at distance l vertically apart. The corresponding stress field is given by Eqs. (13)–(15). Along the plane $y = 0$ the shear stress τ_{xy} of this field does not vanish. Hence, to obtain the stress distribution in a semi-infinite body produced by a vertical wall, superimpose to (13)–(15) the stress distribution produced by the shear stress

$$\tau_{xy}(x, 0) = 2kl\frac{x}{l^2 + x^2}, \tag{B.1}$$

acting over the boundary $y = 0$ of a semi-infinite body. Employing the anti-symmetry of the stress distribution with respect to the y-axis, and its vanishing behavior as $y \to -\infty$, the Airy stress function can be expressed by a Fourier integral

$$\Phi = \int_0^\infty c(\alpha)\, y e^{\alpha y} \cos \alpha x \, d\alpha. \tag{B.2}$$

From the boundary condition (B.1) it follows by a Fourier inversion that $\alpha c(\alpha) = 2kle^{-\alpha l}$, and the Airy stress function becomes

$$\Phi = 2kly\int_0^\infty \frac{1}{\alpha} e^{\alpha(y-l)} \cos \alpha x \, d\alpha. \tag{B.3}$$

This is a divergent integral due to behavior of the integrand at $\alpha = 0$, but its derivatives with respect to x and y are convergent integrals. Hence, by differentiating Eq. (B.3) the stress components are found to be

$$\sigma_x = 2kl\frac{(y-l)^2(2l-y) + x^2(2l-3y)}{\left[x^2 + (y-l)^2\right]^2} \tag{B.4}$$

$$\sigma_y = 2kly\frac{x^2 - (y-l)^2}{\left[x^2 + (y-l)^2\right]^2} \tag{B.5}$$

$$\tau_{xy} = 2klx\frac{x^2 - y^2 + l^2}{\left[x^2 + (y-l)^2\right]^2}. \tag{B.6}$$

The explicit representation of the Airy stress function can be deduced from (B.4)–(B.6) by integration, and is given by

$$\Phi = -kly \ln\left[x^2 + (y-l)^2\right]. \tag{B.7}$$

The total stresses produced by the wall extending from $y = -l$ to $y = -\infty$ in a semi-infinite body are the sums of the corresponding expressions from (13)–(15) and (B.4)–(B.6). This leads to previously obtained expressions (25)–(27).

References

Amodeo, R.J. and N.M. Ghoniem (1990), Dislocation dynamics. II. Applications to the formation of persistent slip bands, planar arrays, and dislocation cells, *Phys. Rev. B* 41, 6968–6976.

Belov, A.Y. (1992), Dislocations emerging at planar boundaries, in: V.L. Indenbom and J. Lothe eds., *Elastic Strain Fields and Dislocation Mobility*, North-Holland, Amsterdam, pp. 391–446.

deWit, R. (1973), Theory of disclinations: II. Continuous and discrete disclinations in anisotropic elasticity, *J. Res. Nat. Bureau of Standards* 77A, No. 1, 49–100.

Dundurs, J. (1969), Elastic interaction of dislocations with inhomogeneities, in: T. Mura, ed., *Mathematical Theory of Dislocations*, ASME, New York, pp. 70–115.

Dundurs, J. and T. Mura (1964), Interaction between an edge dislocation and a circular inclusion, *J. Mech. Phys.* 12, 177–189.

Eshelby, J.D. (1966), A simple derivation of the elastic field of an edge dislocation, *Brit. J. Appl. Phys.* 17, 1131–1135.

Gilman, J.J. (1969), *Micromechanics of Flow in Solids*, McGraw-Hill, New York.

Gutkin, M.Yu. and A.E. Romanov (1991), Straight edge dislocation in a thin two-phase plate, *Phys. Stat. Sol.* (a) 125, 107–125.

Head, A.K. (1953), Edge dislocations in inhomogeneous media, *Proc. Phys. Soc. (London)* B66, 793–801.

Hirth, J.P. and J. Lothe (1968), *Theory of Dislocations*, McGraw-Hill, New York.

Huang, W. and T. Mura (1970), Elastic fields and energies of a circular edge disclination and a straight screw disclination, *J. Appl. Phys.* 41, 5175–5179.

Laird, C. (1983), The application of dislocation concepts in fatigue, in: F.R.N. Nabarro, ed., *Dislocations in Solids*, Vol. 6, North-Holland, Amsterdam, pp. 55–120.

Lee, M.S. and J. Dundurs (1973), Edge dislocation in a surface layer, *Int. J. Engng. Sci.* 11, 87–94.

Li, J.C.M. (1972), Disclination model of high angle grain boundaries, *Surf. Sci.* 31, 12–26.

Lothe, J. (1992), Dislocations interactions with surfaces, interfaces or cracks, in: V.L. Indenbom and J. Lothe, eds., *Elastic Strain Fields and Dislocation Mobility*, North-Holland, Amsterdam, pp. 329–389.

Lubarda, V.A., J.A. Blume and A. Needleman (1993), An analysis of equilibrium dislocation distributions. *Acta metall. mater.* 41, 625–642.

Lubarda, V.A. and D.A. Kouris (1996), Stress fields due to dislocation arrays at interfaces, this issue, Mech. Mater. 23 (1996) 191.

Mura, T. (1989), Impotent dislocation walls, *Mater. Sci. Engng.* A 113, 149–152.

Nabarro, F.R.N. (1967), *Theory of Crystal Dislocations*, Oxford University Press, Oxford.

Nabarro, F.R.N. and E.J. Kostlan (1978), The stress field of a disclination lying in a plate, *J. Appl. Phys.* 49, 5445–5448.

Pond, R.C. (1989), Line defects in interfaces, in: F.R.N. Nabarro, ed., *Dislocations in Solids*, Vol. 8, North-Holland, Amsterdam, pp. 1–66.

Rey, C. and G. Saada (1975), The elastic field of periodic dislocation networks, *Phil. Mag.* 33, 825–841.

Saada, G. (1979), Elastic field of dislocation networks and grain boundaries, *Acta Metall. Mater.* 27, 921–931.

Saada, G. and E. Bouchaud (1993), Dislocation walls, *Acta Metall. Mater.* 41, 2173–2178.